Revision 1

Supplementary Information, Figures, and Tables for the article

Raman analysis of octocoral carbonate ion structural disorder along a natural depth gradient, Kona coast, Hawai‘i

Kyle Conner[1], Shiv Sharma[1], Ryohei Uchiyama[2], Kentaro Tanaka[3], Kotaro Shirai[3], Samuel Kahng[1]

1. School of Ocean and Earth Science and Technology, University of Hawai‘i at Manoa, Honolulu, Hawaii 96822, U.S.A.
2. Graduate School of Science, Hokkaido University, Kita-10 Nishi-8 Kita-ku, Sapporo 060-0810, Japan
3. Atmosphere and Ocean Research Institute, The University of Tokyo, 5-1-5 Kashiwanoha, Kashiwa-shi, Chiba 277-8564, Japan

Keywords: Octocorals, magnesian calcite, carbonate ion disorder, Raman spectroscopy, depth gradient, growth rate kinetics

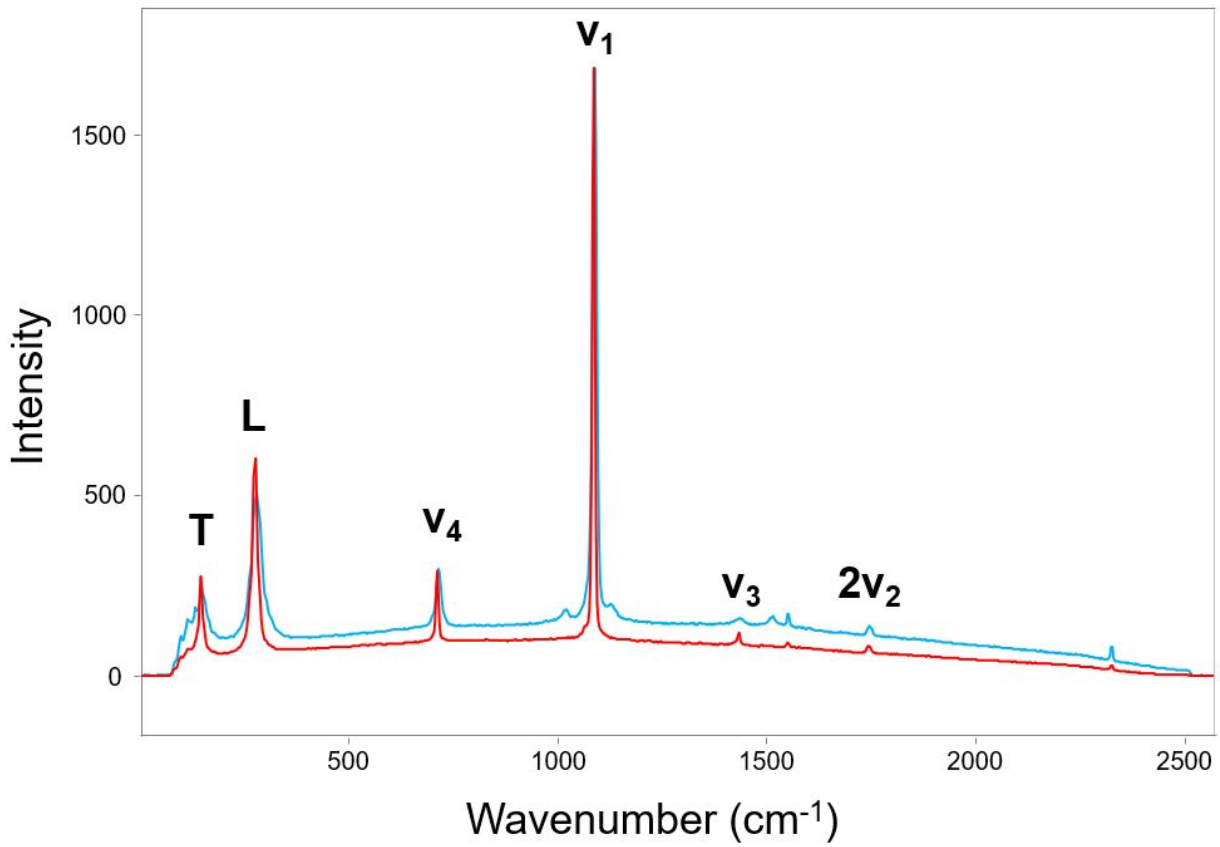

Figure S1. Raman spectra of synthetic (red) and biogenic (blue, *H. imperiale/laauense* from 447 m) calcite with lattice and internal vibration modes labelled.

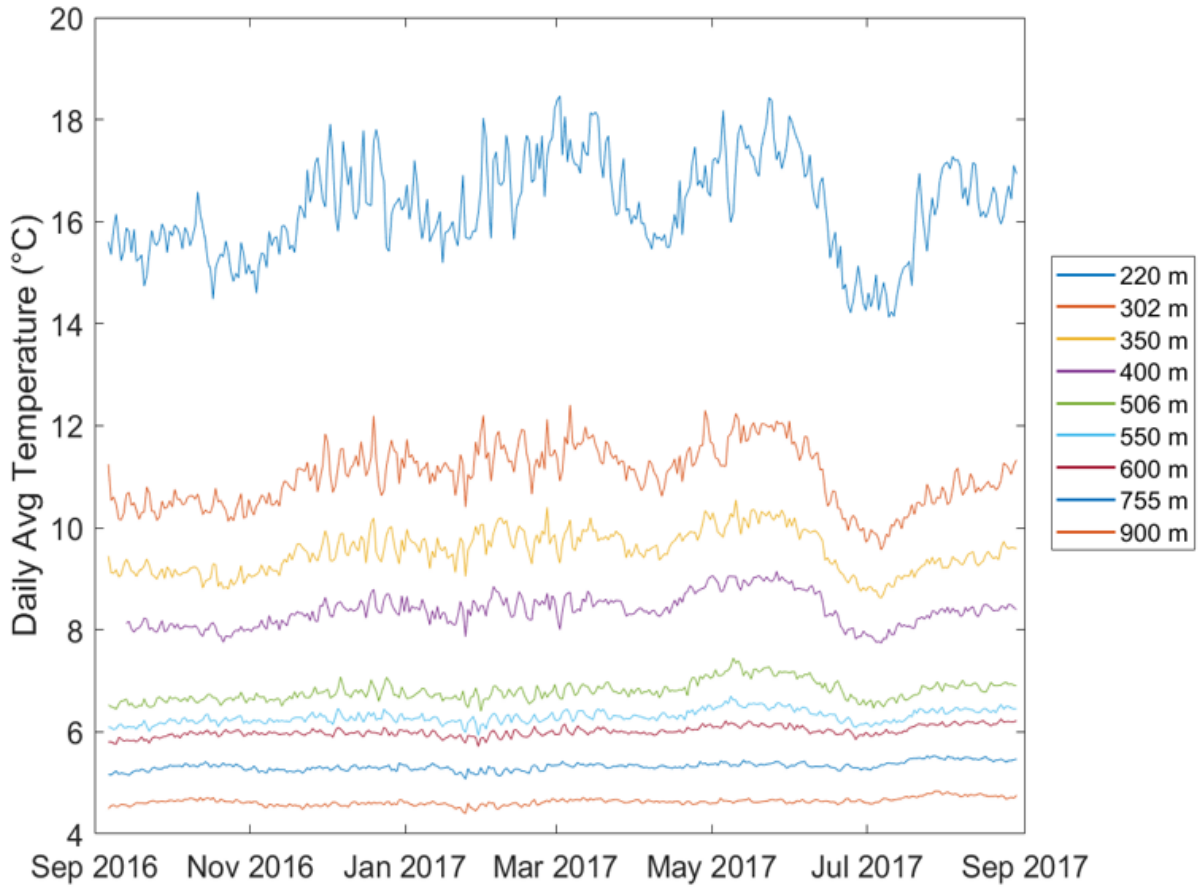

Figure S2: In situ temperature (24-hour averages) along the seafloor at Kailua-Kona for 12 months (Sep 2016–Aug 2017), color coded by depth in meters. The temperature decrease in June is thought to be caused by an anticyclonic mesoscale eddy.

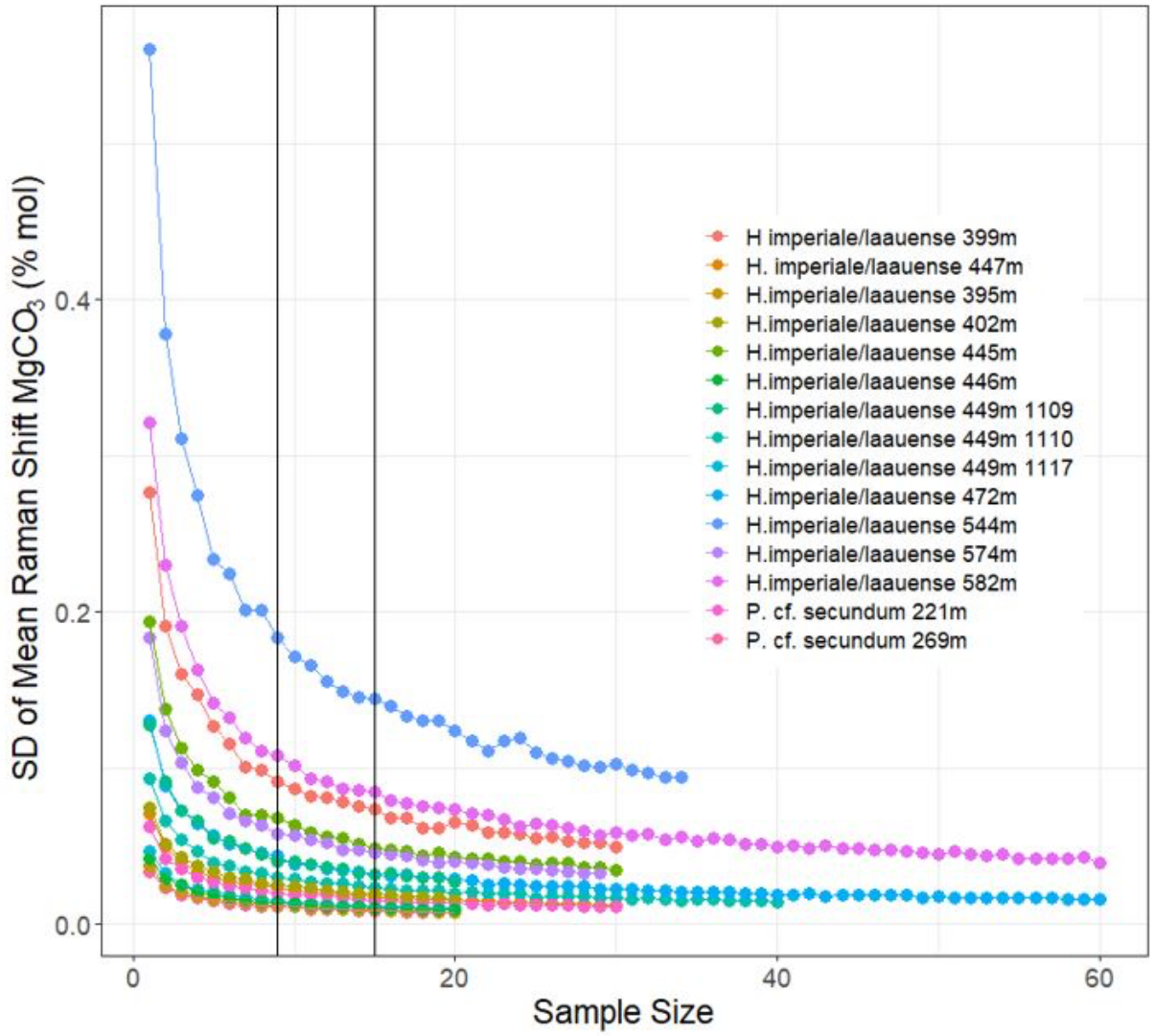

Figure S3: Preliminary sample size analysis of Raman measurements on various octocoral sample surfaces. A bootstrap simulation was conducted containing 1000 iterations where the mean and standard deviation (SD) of Mg content calculated from ν_1 Raman shift measurements were taken for each iteration. The SD of those 1000 mean values represents the bootstrapped standard error of the mean. Black vertical lines represent sample sizes of 9 and 15.

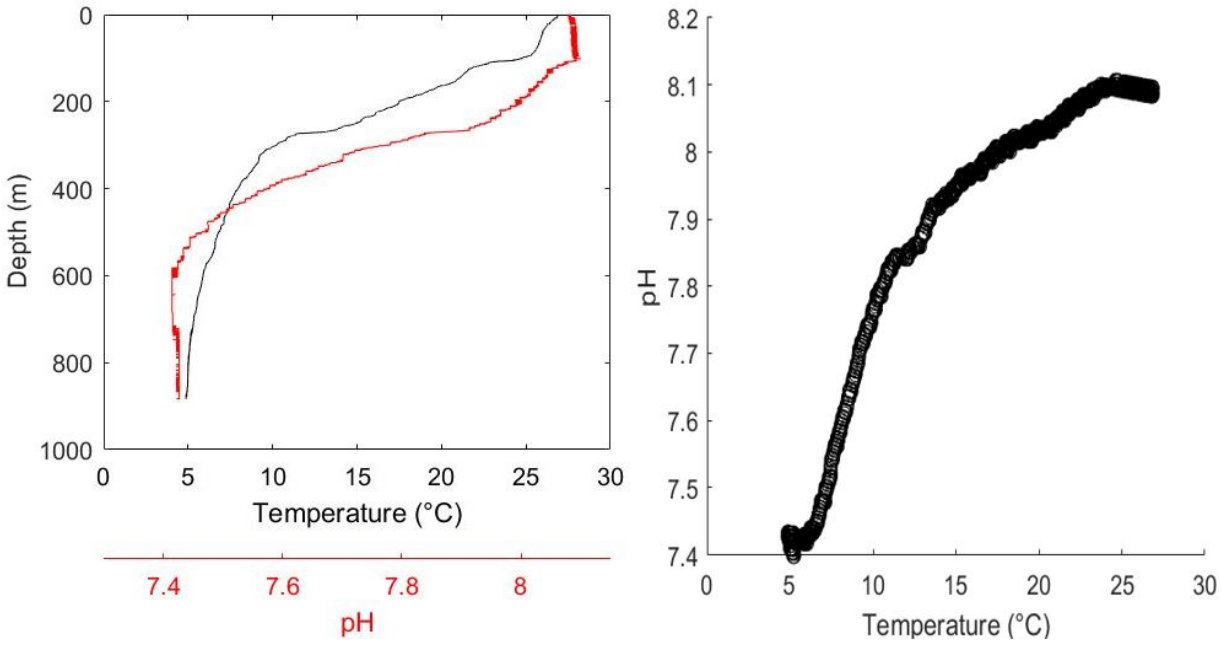

Figure S4: A comparison of temperature and pH data collected from a CTD hydrocast in the Kealakekua Bay site. Collinearity between the two parameters is apparent and can be a common phenomenon in oceanographic depth profile data. Temperature and pH had a correlation of R^2 = 0.95.

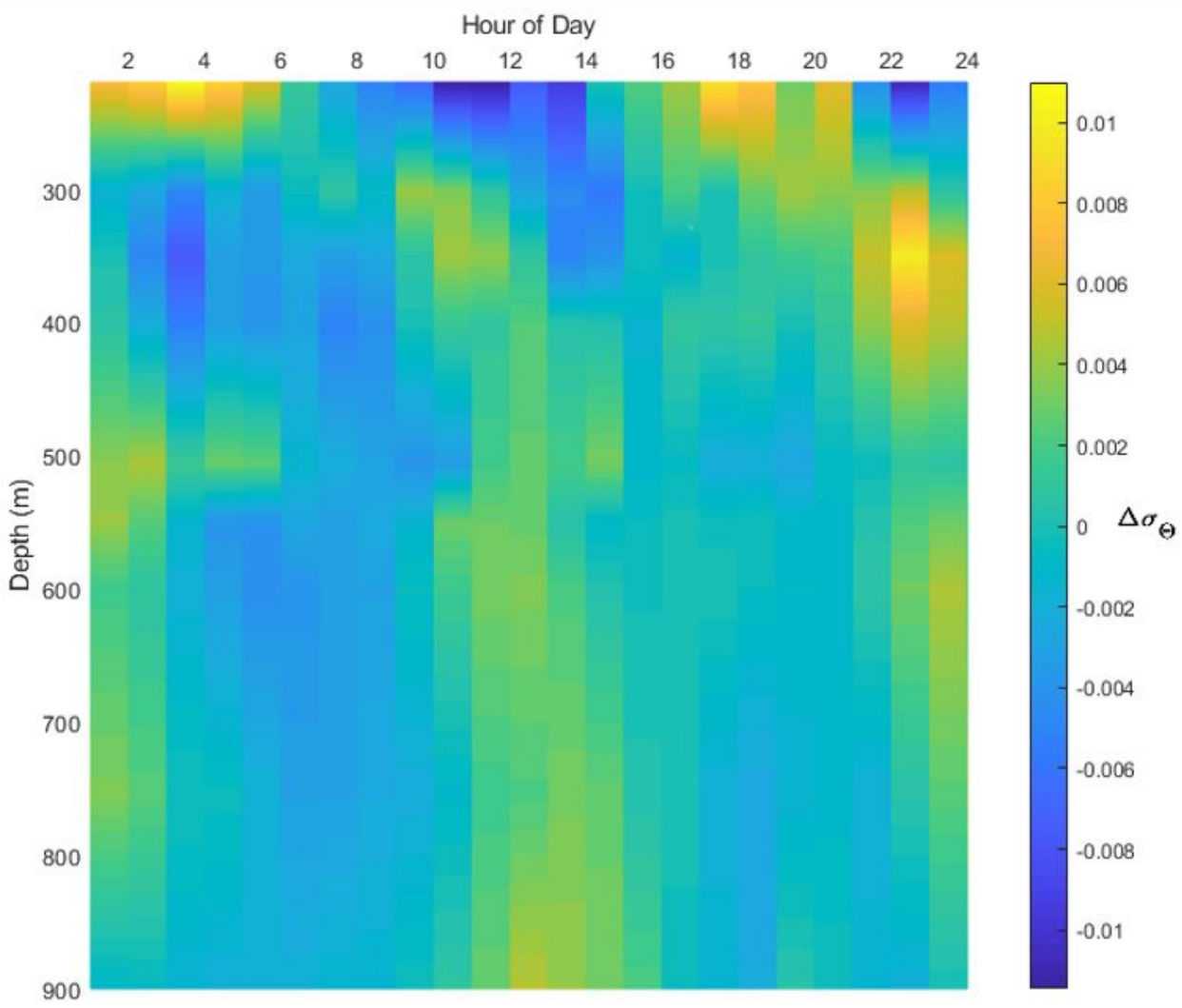

Figure S5: Interpolated color map (24 x 700) of 24-hour averaged change in potential density $\Delta\sigma_\theta$ (difference between measured potential density and average potential density for the entire time-series, kg/m^3) observed at different depths.

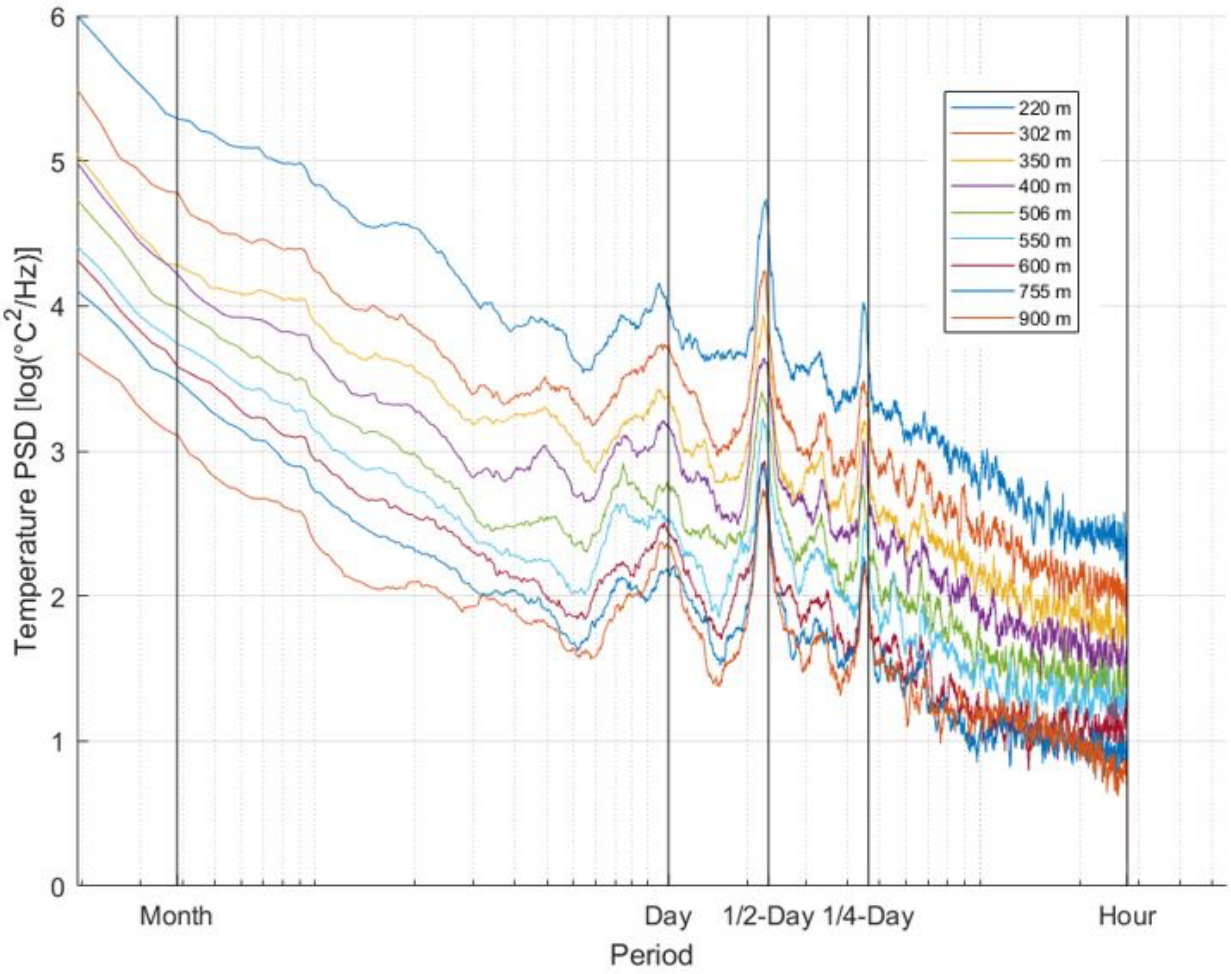

Figure S6: Power spectral density (log-transformed) of in situ temperature data collected from Kailua-Kona for 12 months (Sep 2016 to Aug 2017), color coded by depth in meters. A low pass moving average filter was used to smooth the data. Hourly, quarter day, half day (M_2 semidiurnal), daily, and monthly tidal periods are denoted by the black lines. Tidal fluctuations in temperature appear to attenuate exponentially with depth.

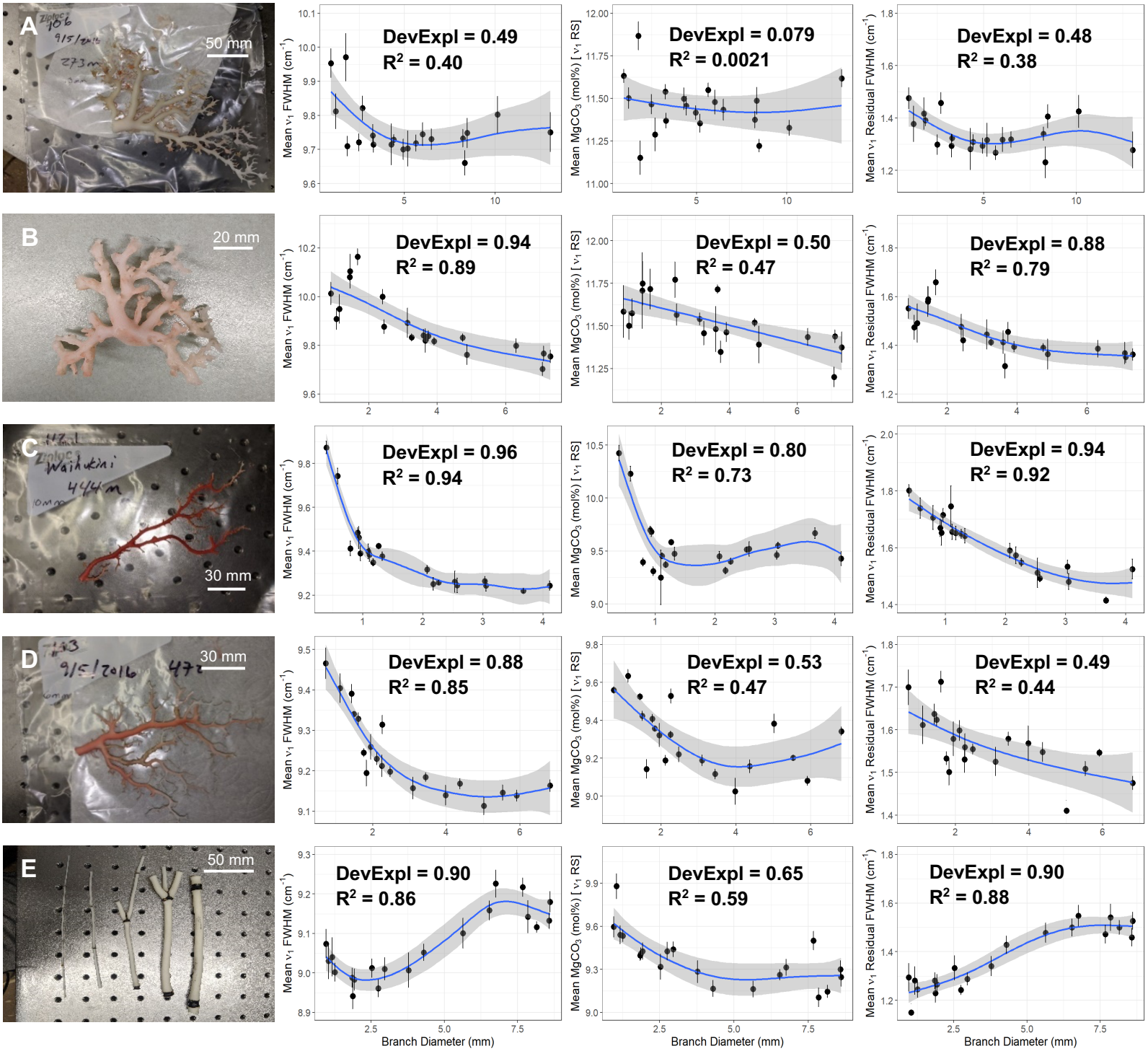

Figure S7. Mean intra-sample octocoral Mg content, ν_1 FWHM, and residual ν_1 FWHM with respect to octocoral branch diameter for five specific samples (each with N = 100) **(a)** *P.* cf. *secundum* from 273 m; **(b)** *C. tortuosum* from 280 m; **(c)** *H. imperiale/laauense* from 444 m; **(d)** *H. imperiale/laauense* from 472 m; **(e)** *Acanella* spp. from 823 m. A general additive model was

used for the trendlines where error bars are ±1 SD, shaded regions are the 95% CI, and DevExpl represents the deviance explained by the model.

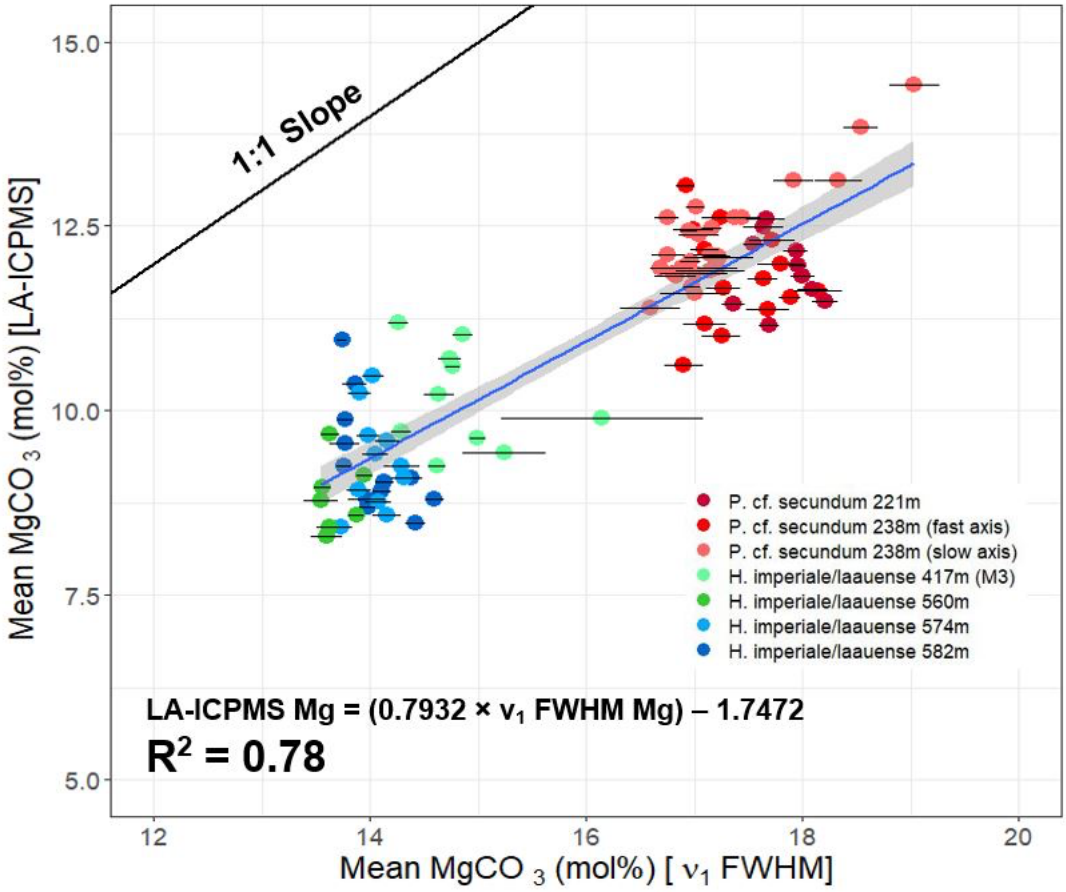

Figure S8: Relationship between Mg content based on ν_1 FWHM (Perrin et al. 2016) and Mg measured using LA-ICPMS (N = 90). The 1:1 line is shown in black. All error bars represent ±1 SD with the shaded regions representing the 95% CI. This figure is similar to Figure 3 in the main text which compares ν_1 Raman shift Mg to LA-ICPMS Mg instead of ν_1 FWHM Mg.

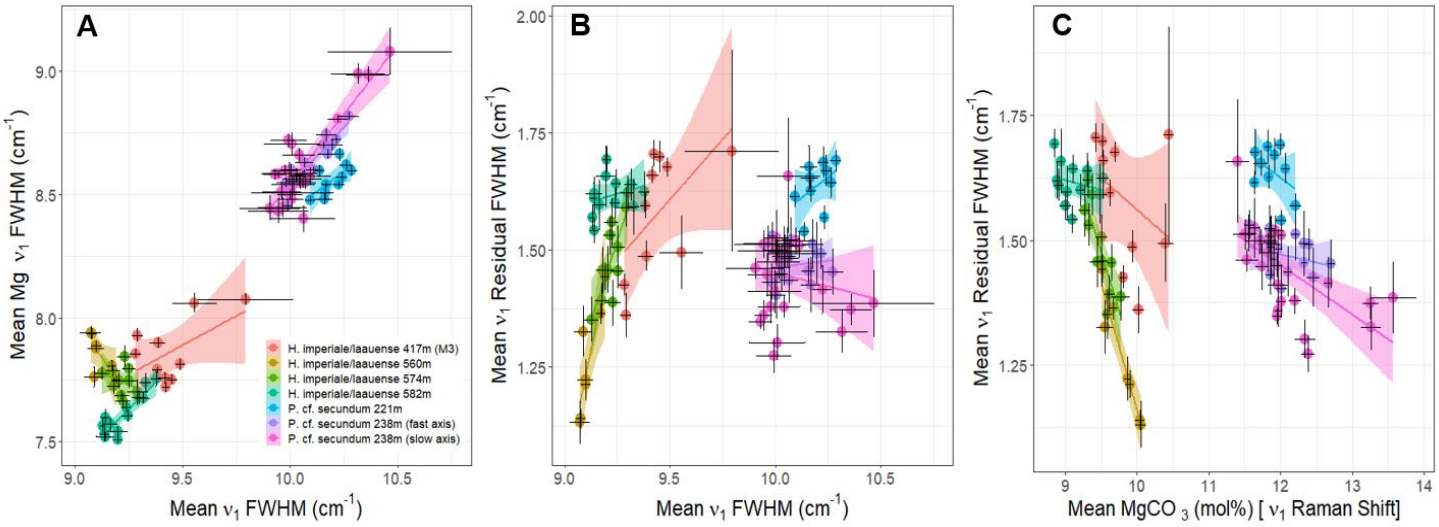

Figure S9: a.) Mean ν_1 FWHM compared to mean ν_1 FWHM contributed by Mg content, **b.)** mean ν_1 FWHM compared to mean residual ν_1 FWHM, and **c.)** mean Mg content (from ν_1 Raman shift) compared to mean residual ν_1 FWHM for the octocorals samples used during the comparison between LA-ICPMS and Raman ν_1 Mg measurements (N = 90). Error bars are ±1 SD while shaded regions are the 95% CI.

Table S1: Linear regression data for ν_1 FWHM in all species with respect to each environmental variable measured. The F-statistic (F) assesses the model's ability to fit the data in comparison to a model without independent variables (where higher values signify a better fit). P-values for statistically significant ($P < 0.05$) models are bolded. No models shown for *C. tortuosum* due to small sample size ($N = 2$).

Species	Environmental Variable	Fitted Coefficients	R	R^2	F	P-value	N
All	Temperature	0.0852x + 8.7000	0.9294	0.8639	164.99	**9.15e-13**	28
All	Salinity	0.7260x – 15.4464	0.3362	0.1130	3.31	0.080	28
All	pH	1.5040x – 1.9593	0.9420	0.8873	204.75	**7.73e-14**	28
All	TA	-0.0052x + 21.3623	-0.4704	0.2213	7.39	**0.012**	28
All	CO_3^{2-}	0.0074x + 8.8407	0.9616	0.9247	319.08	**4.05e-16**	28
All	Ω_{Cal}	0.3132x + 8.8793	0.9612	0.9238	315.32	**4.68e-16**	28
All	Potential Density	-0.5109x + 23.0111	-0.9166	0.8402	136.71	**7.44e-12**	28
Keratoisididae	Temperature	0.0561x + 8.9976	0.6064	0.3677	1.74	0.28	5
Keratoisididae	Salinity	-0.3255x + 20.544	-0.2869	0.0823	0.27	0.64	5
Keratoisididae	pH	1.6252x – 2.7762	0.5713	0.3264	1.45	0.31	5
Keratoisididae	TA	-0.0019x + 13.768	-0.5556	0.3087	1.34	0.33	5
Keratoisididae	CO_3^{2-}	0.0065x + 8.959	0.5401	0.2918	1.24	0.35	5
Keratoisididae	Ω_{Cal}	0.2769x + 8.9949	0.5800	0.3364	1.52	0.31	5
Keratoisididae	Potential Density	-0.2807x + 16.932	-0.5551	0.3082	1.34	0.33	5
H. imperiale/laauense	Temperature	0.0931x + 8.597	0.8137	0.6621	29.39	**7.08e-5**	17
H. imperiale/laauense	Salinity	-0.1219x + 13.461	-0.0985	0.0097	0.15	0.71	17
H. imperiale/laauense	pH	0.7564x – 1.1379	0.7405	0.5483	18.21	**0.00068**	17
H. imperiale/laauense	TA	-0.0051x + 20.902	-0.8623	0.7436	43.50	**8.51e-6**	17
H. imperiale/laauense	CO_3^{2-}	0.0076x + 8.8167	0.8423	0.7094	36.62	**2.22e-5**	17
H. imperiale/laauense	Ω_{Cal}	0.3337x + 8.8333	0.8412	0.7076	36.30	**2.32e-5**	17
H. imperiale/laauense	Potential Density	-0.4942x + 22.513	-0.7275	0.5292	16.86	**0.00093**	17
P. cf. *secundum*	Temperature	0.0708x + 8.8961	0.9969	0.9938	319.40	**0.0031**	4
P. cf. *secundum*	Salinity	0.7668x – 16.469	0.9694	0.9397	31.15	**0.031**	4
P. cf. *secundum*	pH	2.6887x – 11.296	0.9928	0.9857	137.90	**0.0071**	4
P. cf. *secundum*	TA	0.0269x – 51.456	0.9647	0.9307	26.88	**0.035**	4
P. cf. *secundum*	CO_3^{2-}	0.0101x + 8.4541	0.9682	0.9373	29.92	**0.032**	4
P. cf. *secundum*	Ω_{Cal}	0.4123x + 8.5454	0.9680	0.9370	29.77	**0.032**	4
P. cf. *secundum*	Potential Density	-0.5055x + 22.879	-0.9982	0.9963	539.40	**0.0018**	4
Coralliidae	Temperature	0.0930x + 8.6089	0.9685	0.9379	317.36	**3.74e-14**	23
Coralliidae	Salinity	1.0612x – 26.9080	0.4465	0.1994	5.23	**0.033**	23
Coralliidae	pH	1.5823x – 2.5728	0.9731	0.9470	375.13	**7.12e-15**	23
Coralliidae	TA	-0.0108x + 34.1903	-0.6016	0.3619	11.91	**0.0024**	23
Coralliidae	CO_3^{2-}	0.0076x + 8.8106	0.9851	0.9705	691.05	**2.20e-16**	23
Coralliidae	Ω_{Cal}	0.3237x + 8.8459	0.9852	0.9706	694.26	**2.20e-16**	23
Coralliidae	Potential Density	-0.5769x + 24.7354	-0.9691	0.9392	324.52	**3.00e-14**	23

Table S2: Linear regression data for Mg content (from ν_1 Raman shift) in all species with respect to each environmental variable measured. The F-statistic (F) assesses the model's ability to fit the data in comparison to a model without independent variables (where higher values signify a better fit). P-values for statistically significant ($P < 0.05$) models are bolded. No models shown for *C. tortuosum* due to small sample size (N = 2).

Species	Environmental Variable	Fitted Coefficients	R	R^2	F	P-value	N
All	Temperature	0.2362x + 8.0599	0.8348	0.6969	59.78	**3.33e-8**	28
All	Salinity	1.1153x – 28.1403	0.1674	0.0280	0.75	0.39	28
All	pH	4.3643x – 22.9658	0.8861	0.7851	94.99	**3.61e-10**	28
All	TA	-0.0179x + 51.1258	-0.5245	0.2751	9.87	**0.0042**	28
All	CO_3^{2-}	0.0214x + 8.3835	0.8990	0.8082	109.56	**8.12e-11**	28
All	Ω_{Cal}	0.9009x + 8.4991	0.8961	0.8030	105.99	**1.15e-10**	28
All	Potential Density	-1.4333x + 48.1829	-0.8336	0.6949	59.21	**3.64e-8**	28
Keratoisididae	Temperature	0.1326x + 8.8438	0.4394	0.1931	0.72	0.46	5
Keratoisididae	Salinity	-0.0919x + 12.889	-0.0249	0.0006	0.0019	0.97	5
Keratoisididae	pH	4.9526x – 27.295	0.5345	0.2857	1.20	0.35	5
Keratoisididae	TA	-0.0038x + 18.432	-0.3377	0.1140	0.39	0.58	5
Keratoisididae	CO_3^{2-}	0.02425x + 8.1815	0.6186	0.3826	1.86	0.27	5
Keratoisididae	Ω_{Cal}	0.9321x + 8.4541	0.5993	0.3591	1.68	0.29	5
Keratoisididae	Potential Density	-0.5714x + 25.117	-0.3469	0.1203	0.41	0.57	5
H. imperiale/laauense	Temperature	0.4436x + 6.445	0.6946	0.4825	13.99	**0.0020**	17
H. imperiale/laauense	Salinity	-1.1963x + 50.688	-0.1732	0.02999	0.46	0.51	17
H. imperiale/laauense	pH	5.8124x – 33.844	0.6777	0.4593	12.74	**0.0028**	17
H. imperiale/laauense	TA	-0.02282x + 62.047	-0.6959	0.4843	14.09	**0.0019**	17
H. imperiale/laauense	CO_3^{2-}	0.0387x + 7.3198	0.7734	0.5982	22.33	**0.00027**	17
H. imperiale/laauense	Ω_{Cal}	1.7146x + 7.399	0.7745	0.5999	22.49	**0.00026**	17
H. imperiale/laauense	Potential Density	-2.5278x + 77.385	-0.6668	0.4446	12.01	**0.0035**	17
P. cf. *secundum*	Temperature	0.0942x + 9.9246	0.8301	0.6891	4.43	0.17	4
P. cf. *secundum*	Salinity	1.1277x – 27.518	0.8925	0.7966	7.83	0.11	4
P. cf. *secundum*	pH	3.1828x – 13.831	0.7358	0.5414	2.36	0.26	4
P. cf. *secundum*	TA	0.0391x – 77.849	0.8777	0.7695	6.68	0.12	4
P. cf. *secundum*	CO_3^{2-}	0.01475x + 9.1412	0.8882	0.7890	7.48	0.11	4
P. cf. *secundum*	Ω_{Cal}	0.6040x + 9.2755	0.8878	0.7882	7.44	0.11	4
P. cf. *secundum*	Potential Density	-0.6529x + 28.022	-0.8071	0.6514	3.74	0.19	4
Coralliidae	Temperature	0.2471x + 7.9441	0.8514	0.7249	55.34	**2.59e-7**	23
Coralliidae	Salinity	1.8217x – 52.2496	0.2536	0.0643	1.44	0.24	23
Coralliidae	pH	4.4168x – 23.3794	0.8987	0.8077	88.19	**5.75e-9**	23
Coralliidae	TA	-0.0377x + 96.4620	-0.6940	0.4817	19.51	**2.39e-4**	23
Coralliidae	CO_3^{2-}	0.0213x + 8.3983	0.9086	0.8256	99.41	**2.04e-9**	23
Coralliidae	Ω_{Cal}	0.8998x + 8.5015	0.9060	0.8208	96.18	**2.72e-9**	23
Coralliidae	Potential Density	-1.5513x + 51.2822	-0.8622	0.7434	60.83	**1.23e-7**	23

Table S3: Linear regression data for residual ν_1 FWHM in all species with respect to each environmental variable measured. The F-statistic (F) assesses the model's ability to fit the data in comparison to a model without independent variables (where higher values signify a better fit). P-values for statistically significant ($P < 0.05$) models are bolded. No models shown for *C. tortuosum* due to small sample size (N = 2).

Species	Environmental Variable	Fitted Coefficients	R	R^2	F	P-value	N
All	Temperature	0.0034x + 1.4529	0.0782	0.0061	0.016	0.69	28
All	Salinity	0.3489x – 10.4728	0.3388	0.1148	3.37	0.078	28
All	pH	-0.0089x + 1.5495	-0.0117	0.0001	0.0036	0.95	28
All	TA	0.0011x – 0.9377	0.2000	0.0400	1.08	0.31	28
All	CO_3^{2-}	-4.5794e-7x + 1.4820	-1.244e-4	1.5466e-8	4.02e-7	1.00	28
All	Ω_{Cal}	8.8272e-4x + 1.4805	0.0057	3.2263e-5	8.39e-4	0.98	28
All	Potential Density	-0.0142x + 1.8607	-0.0536	0.0029	0.075	0.79	28
Keratoisididae	Temperature	0.008294x + 1.4894	0.1011	0.01022	0.031	0.87	5
Keratoisididae	Salinity	-0.2864x + 11.374	-0.2850	0.08123	0.27	0.64	5
Keratoisididae	pH	-0.157x + 2.7192	-0.0623	0.003883	0.012	0.92	5
Keratoisididae	TA	-0.0005372x + 2.7861	-0.1772	0.03141	0.097	0.78	5
Keratoisididae	CO_3^{2-}	-0.002201x + 1.6865	-0.2065	0.04263	0.13	0.74	5
Keratoisididae	Ω_{Cal}	-0.05799x + 1.6251	-0.1371	0.0188	0.057	0.83	5
Keratoisididae	Potential Density	-0.07360x + 3.5263	-0.1643	0.02713	0.083	0.79	5
H. imperiale/laauense	Temperature	-0.06367x + 1.9333	-0.4178	0.1746	3.17	0.095	17
H. imperiale/laauense	Salinity	0.3129x – 9.2508	0.1898	0.03603	0.56	0.47	17
H. imperiale/laauense	pH	-0.9118x + 8.2972	-0.4455	0.1984	3.71	0.073	17
H. imperiale/laauense	TA	0.002997x – 5.4104	0.3830	0.1467	2.58	0.13	17
H. imperiale/laauense	CO_3^{2-}	-0.006112x + 1.8425	-0.5118	0.2619	5.32	**0.036**	17
H. imperiale/laauense	Ω_{Cal}	-0.2717x + 1.8313	-0.5142	0.2644	5.39	**0.035**	17
H. imperiale/laauense	Potential Density	0.40212x – 9.3007	0.4445	0.1975	3.69	0.074	17
P. cf. *secundum*	Temperature	0.03881x + 0.9957	0.8441	0.7125	4.96	0.16	4
P. cf. *secundum*	Salinity	0.3861x – 11.73	0.7540	0.5685	2.63	0.25	4
P. cf. *secundum*	pH	1.5968x – 11.042	0.9109	0.8297	9.74	0.089	4
P. cf. *secundum*	TA	0.01369x – 29.649	0.7578	0.5742	2.70	0.24	4
P. cf. *secundum*	CO_3^{2-}	0.005082x + 0.8160	0.7551	0.5702	2.65	0.24	4
P. cf. *secundum*	Ω_{Cal}	0.2082x + 0.8619	0.7552	0.5703	2.65	0.24	4
P. cf. *secundum*	Potential Density	-0.2832x + 8.8181	-0.8640	0.7464	5.89	0.14	4
Coralliidae	Temperature	0.007341x + 1.4029	0.1773	0.0314	0.68	0.42	23
Coralliidae	Salinity	0.4433x – 13.7154	0.4326	0.1871	4.83	**0.039**	23
Coralliidae	pH	0.0499x + 1.0899	0.0711	0.0051	0.11	0.75	23
Coralliidae	TA	0.0024x – 3.9846	0.3073	0.0944	2.19	0.15	23
Coralliidae	CO_3^{2-}	0.0003x + 1.4476	0.0754	0.0057	0.12	0.73	23
Coralliidae	Ω_{Cal}	0.0117x + 1.4470	0.0822	0.0068	0.14	0.71	23
Coralliidae	Potential Density	-0.0389x + 2.4993	-0.1515	0.0229	0.49	0.49	23

Table S4: Linear model statistics of the Mg (ν_1 Raman shift) and ν_1 FWHM relationships obtained from the five octocoral specimens used during the intra-sample variability measurements. The F-statistic (F) assesses the model's ability to fit the data in comparison to a model without independent variables (where higher values signify a better fit). P-values for statistically significant ($P < 0.05$) models are bolded. All specimens had N = 100.

Specimen	Model Variables	Fitted Coefficients	R	R^2	F	P-value
P. cf. *secundum* 273 m	FWHM vs. Mg FWHM	0.3485x + 5.0167	0.5378	0.2892	7.33	**0.014**
P. cf. *secundum* 273 m	FWHM vs. Residual FWHM	0.6515x – 5.0167	0.7662	0.5871	25.59	**8.17e-5**
P. cf. *secundum* 273 m	Mg vs. Residual FWHM	-0.0545xx + 1.9651	0.1261	0.0159	0.29	0.60
C. tortuosum 280 m	FWHM vs. Mg FWHM	0.3187x + 5.2919	0.8170	0.6675	36.14	**1.10e-5**
C. tortuosum 280 m	FWHM vs. Residual FWHM	0.6813x – 5.2919	0.9496	0.9018	165.20	**1.66e-10**
C. tortuosum 280 m	Mg vs. Residual FWHM	0.3602x – 2.7067	0.5791	0.3354	9.92	**0.0055**
H. imperiale/laauense 444 m	FWHM vs. Mg FWHM	0.5029x + 3.0478	0.8203	0.6729	37.03	**9.47e-6**
H. imperiale/laauense 444 m	FWHM vs. Residual FWHM	0.4971x – 3.0478	0.8171	0.6677	36.17	**1.09e-5**
H. imperiale/laauense 444 m	Mg vs. Residual FWHM	0.1216x + 0.4521	0.3451	0.1191	2.43	0.14
H. imperiale/laauense 472 m	FWHM vs. Mg FWHM	0.4448x + 3.5648	0.7212	0.5202	19.52	**0.00033**
H. imperiale/laauense 472 m	FWHM vs. Residual FWHM	0.5552x – 3.5648	0.7926	0.6282	30.41	**3.09e-5**
H. imperiale/laauense 472 m	Mg vs. Residual FWHM	0.0622x + 0.9858	0.1510	0.0228	0.42	0.53
Acanella spp. 823 m	FWHM vs. Mg FWHM	-0.2563x + 10.0231	0.3291	0.1083	2.19	0.16
Acanella spp. 823 m	FWHM vs. Residual FWHM	1.2563x -10.0231	0.8630	0.7448	52.24	**9.70e-7**
Acanella spp. 823 m	Mg vs. Residual FWHM	-0.5134x + 6.1823	0.7603	0.5780	24.65	**0.0001**

Table S5: Linear model statistics of the Mg (from ν_1 Raman shift) and ν_1 FWHM relationships obtained from the octocorals samples used during the comparison between LA-ICPMS and Raman ν_1 Mg measurements. The F-statistic (F) assesses the model's ability to fit the data in comparison to a model without independent variables (where higher values signify a better fit). P-values for statistically significant ($P < 0.05$) models are bolded.

Specimen	Model Variables	Fitted Coefficients	R	R^2	F	P-value	N
P. cf. *secundum* 221 m	FWHM vs. Mg FWHM	0.6457x + 1.9757	0.6560	0.4303	6.04	**0.039**	10
P. cf. *secundum* 221 m	FWHM vs. Residual FWHM	0.3544x – 1.9770	0.4308	0.1856	1.82	0.21	10
P. cf. *secundum* 221 m	Mg vs. Residual FWHM	-0.3330x + 4.4880	0.3985	0.1588	1.51	0.25	10
P. cf. *secundum* 238 m (fast axis)	FWHM vs. Mg FWHM	0.9422x – 0.8843	0.9184	0.8434	64.65	**3.57e-6**	14
P. cf. *secundum* 238 m (fast axis)	FWHM vs. Residual FWHM	0.0574x + 0.8878	0.1400	0.0196	0.24	0.63	14
P. cf. *secundum* 238 m (fast axis)	Mg vs. Residual FWHM	-0.1053x + 2.3768	0.2632	0.0693	0.89	0.36	14
P. cf. *secundum* 238 m (slow axis)	FWHM vs. Mg FWHM	1.1172x – 2.6233	0.8728	0.7617	76.72	**6.12e-9**	26
P. cf. *secundum* 238 m (slow axis)	FWHM vs. Residual FWHM	-0.1173x + 2.6248	0.1844	0.034	0.85	0.37	26
P. cf. *secundum* 238 m (slow axis)	Mg vs. Residual FWHM	-0.3180x + 4.1835	0.6410	0.4109	16.74	**0.0004**	26
H. imperiale/laauense 417 m (M3)	FWHM vs. Mg FWHM	0.4756x + 3.3721	0.5542	0.3071	3.55	0.096	10
H. imperiale/laauense 417 m (M3)	FWHM vs. Residual FWHM	0.5130x – 3.2649	0.5816	0.3383	4.089	0.078	10
H. imperiale/laauense 417 m (M3)	Mg vs. Residual FWHM	-0.3646x + 4.4492	0.3548	0.1259	1.15	0.31	10
H. imperiale/laauense 560 m	FWHM vs. Mg FWHM	-1.2001x + 18.7908	0.7099	0.5040	5.08	0.074	7
H. imperiale/laauense 560 m	FWHM vs. Residual FWHM	2.2009x – 18.7982	0.8797	0.7738	17.10	**0.0090**	7
H. imperiale/laauense 560 m	Mg vs. Residual FWHM	-1.4201x + 12.4135	0.9595	0.9206	57.95	**0.0006**	7
H. imperiale/laauense 574 m	FWHM vs. Mg FWHM	-0.3694x + 11.1474	0.3321	0.1103	1.12	0.32	10
H. imperiale/laauense 574 m	FWHM vs. Residual FWHM	1.3691x – 11.1441	0.7937	0.6300	15.33	**0.0035**	10
H. imperiale/laauense 574 m	Mg vs. Residual FWHM	-1.2985x – 11.5331	0.8374	0.7012	21.12	**0.0013**	10
H. imperiale/laauense 582 m	FWHM vs. Mg FWHM	0.8690x – 0.4077	0.8826	0.7789	35.22	**0.0001**	12
H. imperiale/laauense 582 m	FWHM vs. Residual FWHM	0.1310x + 0.4076	0.2724	0.0742	0.80	0.39	12
H. imperiale/laauense 582 m	Mg vs. Residual FWHM	-0.1036x + 2.4030	0.2121	0.0450	0.47	0.51	12

Table S6: Mg-temperature relationships from this study and other relevant octocoral or inorganic calcite studies. Numbers in the parentheses represent the 95% CI.

Study	Taxon	Fitted Model Mg/Ca (mmol/mol) = A×T(°C) + B	Temp. Range (°C)	N
This Study	Coralliidae & Keratoisididae	$2.94(\pm0.75) \times T(°C) + 87.02(\pm6.74)$	5-16.4	28
This Study	Coralliidae	$3.08(\pm0.82) \times T(°C) + 85.58(\pm7.66)$	6-16.4	23
This Study	Keratoisididae	$1.64(\pm3.84) \times T(°C) + 96.87(\pm26.38)$	5-8.4	5
Weinbauer et al. 2000	Coralliidae (*C. rubrum*)	$5.03(\pm1.14) \times T(°C) + 39.0(\pm16.8)$	13-16	3
Chave 1954 Weinbauer et al. 2000 Yoshimura et al. 2011 Thresher et al. 2016	Coralliidae (*Corallium* spp.)	$3.08(\pm0.56) \times T(°C) + 70.9(\pm7.32)$	0-19.5	17
Chaabane et al. 2019	Coralliidae (*C. rubrum*)	$2.89(\pm0.59) \times T(°C) + 73.98(\pm9.09)$	13.8-16.8	12
Yoshimura et al. 2011 Vielzeuf et al. 2013 Chaabane et al. 2019	Coralliidae (*Corallium* spp.)	$3.71(\pm0.23) \times T(°C) + 66.89(\pm3.21)$	2.5-19.5	24
Thresher et al. 2016	Isididae*	$2.93(\pm0.25) \times T(°C) + 72.1(\pm2.46)$	-1.9-26.8	73
Mucci 1987	Inorganic Mg-calcite	$3.16(\pm0.28) \times T(°C) + 42(\pm0.92)$	5-40	3

Note: Compiled Mg-temperature data was generated by Thresher et al. (2016) and Chaabane et al. (2019), respectively. *Samples from Thresher et al. (2016) now consist of various octocoral families including both Isididae and Keratoisididae, according to Heestand Saucier et al. (2021).

References Cited

Bischoff, W.D., Sharma, S.K., and MacKenzie, F.T. (1985) Carbonate ion disorder in synthetic and biogenic magnesian calcites: a Raman spectral study. American Mineralogist, 70, 581-589.

Borromeo, L., Zimmermann, U., Andò, S., Coletti, G., Bersani, D., Basso, D., Gentile, P., Schulz, B., and Garzanti, E. (2017) Raman spectroscopy as a tool for magnesium estimation in Mg-calcite. Journal of Raman Spectroscopy, 48, 983-992.

Chaabane, S., López Correa, M., Ziveri, P., Trotter, J., Kallel, N., Douville, E., McCulloch, M., Taviani, M., Linares, C., and Montagna, P. (2019) Elemental systematics of the calcitic skeleton of Corallium rubrum and implications for the Mg/Ca temperature proxy. Chemical Geology, 52, 237-258.

Chave, K.E. (1954) Aspects of biogeochemistry of magnesium 1. Calcareous marine organisms. Journal of Geology, 62, 266–283.

Comeau, S., Cornwall, C.E., DeCarlo, T.M., Krieger, E., and McCulloch, M.T. (2018) Similar controls on calcification under ocean acidification across unrelated coral reef taxa. Global Change Biology, 24, 4857-4868.

Cornwall, C., Comeau, S., DeCarlo, T., Moore, B., D'alexis, Q., and McCulloch, M. (2018) Resistance of corals and coralline algae to ocean acidification: physiological control of calcification under natural pH variability. Proceedings of the Royal Society B: Biological Sciences, 285, 20181168.

Cornwall, C., Comeau, S., DeCarlo, T.M., Larcombe, E., Moore, B., Giltrow, K., Puerzer, F., D'Alexis, Q., and McCulloch, M.T. (2020) A coralline alga gains tolerance to ocean acidification over multiple generations of exposure. Nature Climate Change, 10, 143-146.

DeCarlo, T., D'Olivo, J., Foster, T., Holcomb, M., Becker, T., and McCulloch, M. (2017) Coral calcifying fluid aragonite saturation states derived from Raman spectroscopy. Biogeosciences, 14, 5253-5269.

DeCarlo, T.M., Ren, H., and Farfan, G.A. (2018) The origin and role of organic matrix in coral calcification: Insights from comparing coral skeleton and abiogenic aragonite. Frontiers in Marine Science, 5, 170.

DeCarlo, T.M., Comeau, S., Cornwall, C.E., Gajdzik, L., Guagliardo, P., Sadekov, A., Thillainath E.C., Trotter, J., McCulloch, M.T. (2019) Investigating marine bio calcification mechanisms in a changing ocean with in vivo and high-resolution ex vivo Raman spectroscopy. Global Change Biology, 25, 1877-1888.

Farfan, G.A., Cordes, E.E., Waller, R.G., DeCarlo, T.M., and Hansel, C.M. (2018) Mineralogy of Deep-Sea Coral Aragonites as a Function of Aragonite Saturation State. Frontiers in Marine Science, 5, 473.

Farfan, G.A., Apprill, A., Cohen, A., DeCarlo, T.M., Post, J.E., Waller, R.G., and Hansel, C.M. (2021) Crystallographic and chemical signatures in coral skeletal aragonite. Coral Reefs, 41, 19-34.

Farmer, J.R., Hönisch, B., Robinson, L.F., and Hill, T.M. (2015) Effects of seawater-pH and

biomineralization on the boron isotopic composition of deep-sea bamboo corals. Geochimica et Cosmochimica Acta, 155, 86-106.

Heestand Saucier, E., France, S.C., and Watling, L. (2021) Toward a revision of the bamboo corals: Part 3, deconstructing the Family Isididae. Zootaxa, 5047, 247-272.

Hennige, S.J., Wicks, L.C., Kamenos, N.A., Perna, G., Findlay, H.S., and Roberts, J.M. (2015) Hidden impacts of ocean acidification to live and dead coral framework. Proceedings of the Royal Society of London B: Biological Sciences, 282, 20150990.

Kamenos, N.A., Burdett, H.L., Aloisio, E., Findlay, H.S., Martin, S., Longbone, C., Dunn, J., Widdicombe, S., and Calosi, P. (2013) Coralline algal structure is more sensitive to rate, rather than the magnitude, of ocean acidification. Global Change Biology, 19, 3621-3628.

Kamenos, N.A., Perna, G., Gambi, M.C., Micheli, F., and Kroeker, K.J. (2016) Coralline algae in a naturally acidified ecosystem persist by maintaining control of skeletal mineralogy and size. Proceedings of the Royal Society of London B: Biological Sciences, 283, 20161159.

Mucci, A. (1987) Influence of temperature on the composition of magnesian calcite overgrowths precipitated from seawater. Geochimica et Cosmochimica Acta, 51, 1977-1984.

Perrin, J., Vielzeuf, D., Laporte, D., Ricolleau, A., Rossman, G.R., and Floquet, N. (2016) Raman characterization of synthetic magnesian calcites. American Mineralogist, 101, 2525-2538.

Pauly, M., Kamenos, N.A., Donohue, P., and LeDrew, E. (2015) Coralline algal Mg-O bond strength as a marine pCO_2 proxy. Geology, 43, 267-270.

Thresher, R.E., Fallon, S.J., and Townsend, A.T. (2016) A “core-top” screen for trace element proxies of environmental conditions and growth rates in the calcite skeletons of bamboo corals (Isididae). Geochimica et Cosmochimica Acta, 193, 75-99.

Urmos, J., Sharma, S.K., and Mackenzie, F.T. (1991) Characterization of some biogenic carbonates with Raman spectroscopy. American Mineralogist, 76, 641-646.

Vielzeuf, D., Garrabou, J., Gagnon, A., Ricolleau, A., Adkins, J., Günther, D., Hametner, K., Devidal, J-L., Reusser, E., and Perrin, J. (2013) Distribution of sulphur and magnesium in the red coral. Chemical Geology, 355, 13-27.

Vielzeuf, D., Gagnon, A.C., Ricolleau, A., Devidal, J-L., Balme-Heuze, C., Yahiaoui, N., Fonquernie, C., Perrin, J., Garrabou, J., and Montel, J-M. (2018) Growth kinetics and distribution of trace elements in precious corals. Frontiers in Earth Science, 6, 167.

Wang, D., Hamm, L.M., Bodnar, R.J., and Dove, P.M. (2012) Raman spectroscopic characterization of the magnesium content in amorphous calcium carbonates. Journal of Raman Spectroscopy, 43, 543-548.

Weinbauer, M., Brandstätter, F., and Velimirov, B. (2000) On the potential use of magnesium and strontium concentrations as ecological indicators in the calcite skeleton of the red coral (Corallium rubrum). Marine Biology, 137, 801-809.

Yoshimura, T., Tanimizu, M., Inoue, M., Suzuki, A., Iwasaki, N., and Kawahata, H. (2011) Mg isotope fractionation in biogenic carbonates of deep-sea coral, benthic foraminifera, and hermatypic coral. Analytical and Bioanalytical Chemistry, 401, 2755-2769.